Comparison of a theoretical impedance model with experimental measurements of pulsatile blood flow

R.L. Gaw, B.H. Cornish and B.J. Thomas

School of Physical and Chemical Sciences, Queensland University of Technology, Brisbane, Australia

Abstract— **The velocity dependent changes in the impedance of flowing blood have been widely reported in the literature. These changes have been suggested as a source of the impedance change of the thorax measured during Impedance Cardiography techniques. In this study, a theoretical model incorporating red blood cell orientation, was developed to predict the impedance of pulsatile blood as it flows through rigid tubes. Experimental measurements were recorded for comparisons with the theoretical model. Bovine blood was pumped through rigid tubes in a mock circulatory system and its impedance and velocity were measured. Experimental and theoretical impedance and velocity waveforms are presented for a range of cardiac parameters such as pulse rate, stroke volume and systolic/diastolic ratio. Comparisons show that the theoretical model successfully simulated features of the experimental waveforms. These were: 1) a difference between impedance during accelerating and decelerating flow at the same velocity, 2) an instantaneous impedance response to acceleration, and 3) a decay in impedance during deceleration to zero flow. Both the modelled and experimental impedance data also indicate a good cross correlation with the velocity (r=0.73 and 0.65 respectively at a pulse rate of 70 beats per minute). These results theoretically and experimentally demonstrate that the impedance of flowing blood contains information related to the velocity of the blood and may prove useful in understanding impedance variations in Impedance Cardiography.**

Keywords— **Bioimpedance, Red Blood Cell Orientation, Mathematical Model, Pulsatile Blood Flow.**

I. Introduction

The origin of the Impedance Cardiogram (ICG) is not well agreed upon in the literature [1]-[6]. In addition to the accepted blood volume changes, multiple other factors are reported as the source of the impedance change. One of these is the velocity dependent changes in the resistivity of blood [7]-[16]. Previous studies suggest that this effect is sufficient to be observed in Impedance Cardiography (IC) measurements [7]-[9].

These flow dependant impedance changes are thought to be caused, at least in part, by changes in the alignment of the red blood cells (RBCs) in response to changing shear forces [7]. As the shear force increases, cells align with the minimum cross sectional area facing the direction of flow. This minimises the shearing stress across the surface of the cell and will alter the impedance of blood.

Published literature concerning the varying electrical impedance of blood has primarily investigated blood in *constant* flow. However, blood flow through the body is pulsatile in nature and these studies are not able to adequately explain blood impedance changes under physiological flow conditions. Although it has been demonstrated experimentally that the resistivity of blood changes during the cardiac cycle [16], the variation of blood resistivity in pulsatile flow remains largely unexplored. Certainly, no studies have been reported which theoretically model the impedance of pulsatile blood flow. This study investigates the flow dependence of the electrical impedance of blood during pulsatile flow through rigid tubes, using theoretical modelling and experimental data collection.

II. Theory and methods

A. Theoretical Model

The conductivity of blood has previously been quantitatively modelled under the condition of steady laminar flow through rigid cylindrical tubes [15]. This was achieved by extending the Maxwell-Fricke theory to include orientation and deformation of ellipsoidal particles induced by shear stresses. In this previous model, it is the shear stress experienced by the RBC's and its variation across the radius that is the most important factor in modelling the conductivity of blood flow. Because of this, the steady state model can be shown to fail when applied to pulsatile blood flow. This is because the velocity profiles of the two conditions of flow (from which the shear rate (γ) and shear stress (τ) are derived) are very different in steady state and pulsatile flow. While the steady radial flow profile is parabolic, the pulsatile flow profile is largely flattened in the central axial region. For pulsatile flow, this results in low shear rates in the inner tube while high shear rates are experienced near the walls of the tubes.

However, the previous model reported in [15] was shown to successfully predict the conductivity of blood in constant flow and so the methodology used was replicated in this paper for the condition of pulsatile flow. In addition, realis-

Hermann Scharfetter, Robert Merva (Eds.): ICEBI 2007, IFMBE Proceedings 17, pp. 32–35, 2007
www.springerlink.com

tic cell orientation dynamics were also incorporated to extend the previous model.

To model the impedance of blood, each RBC was assumed to be enclosed in a small control volume containing the cell and surrounding plasma and positioned at a distance r along the radius. The conductivity of this control volume was calculated and integrated over the cross sectional area of the tube to find the bulk impedance. Constant flow parameters for bovine blood were used.

Step 1. The shear stress profile, τ(r), was derived from the velocity profile, v(r). This was achieved using the methods outlined in [17] and [18] and is given in equation 1.

$$\tau(r)\ (N.m^{-2}) = \frac{\eta A}{\mathrm{i}\omega\rho}\cdot\left[\frac{\alpha \mathrm{i}^{\frac{3}{2}} J_1\left(\alpha\frac{r}{R}\mathrm{i}^{\frac{3}{2}}\right)}{J_0\left(\alpha \mathrm{i}^{\frac{3}{2}}\right)}\right]\cdot \mathrm{e}^{\mathrm{i}\omega t} \quad (1)$$

Where A is the pressure coefficient (dyn.cm^{-2}), ω is the angular frequency of the driving pressure gradient (rad.s^{-1}), r is the radial distance from the axial of the tube (cm), R is the radius of the tube (cm), ρ is the density of blood (1.055 g.cm^{-3}), J_0 and J_1 are Bessel functions, t is time (s), η is the viscosity of blood ($\eta_{bl} = \eta_{pl}(1+2.5\times h+7.37\times h^{-2})$, h = haematocrit, η_{pl} = 1.72 x10^{-3} Pa.s) and α is Womersley's number, calculated using (2).

$$\alpha = R\sqrt{\frac{\omega\rho}{\eta}} \quad (2)$$

The spatial average velocity is the average velocity of all lamina flowing through the cross section of the tube and is also calculated from the velocity profile.

Step 2. The cell deformation induced by this shear stress was calculated for the present study using the method presented in [15]. The amount of deformation is indicated by a change in the ratio of the short to long axes of the cell (a_d/b_d) in (3).

$$\frac{a_d(r)}{b_d(r)} = \frac{a_0}{b_0}\left[1+\frac{\tau(r)b_0}{4\mu}\right] \quad (3)$$

Where a_0/b_0 is the initial axis ratio (0.22), b_0 is the original long axis length (5.5 μm) and μ is the surface shear modulus of the cell membrane (1.5x10^{-5} N.m^{-1}).

Step 3. The orientation of the red blood cells across the radius was determined. Hoetink et al [15] use a simple linear relationship based on the shear rate, however, the characteristics of the cell orientation process are difficult to account for. For time varying flow, it has been reported that the times taken by RBCs to align with the flow and the time taken to disorientate also differ largely [8], [19]. This can be described as a first order kinetic process which is dependent on the shear rate experienced by the cells. Equation (4) shows an approximate expression for the orientation rate as a function of shear rate across the radius of the tube presented in [20].

$$f(r) = \frac{n}{n_0} = \frac{\tau_o^{-1}(r)}{\tau_d^{-1}(r)+\tau_o^{-1}(r)} \quad (4)$$

Where n is the number of RBCs with stable orientation per unit volume (in this case, assumed to be oriented parallel to the flow), n_o is the total number of RBCs per unit volume, $\tau_o = 1/\gamma$ and $\tau_d = 1/\sqrt{\gamma}$.

Step 4. The conductivity of a representative control volume was then calculated using the highly cited Maxwell-Fricke equations as followed in [15]. For a single control volume located at a distance r from the axis, the conductivity was calculated using (5).

$$\frac{\sigma_{cv}}{\sigma_{pl}} = \frac{1-h}{1+(C-1)\cdot h} \quad (5)$$

Where σ_{cv} and σ_{pl} are the conductivities (σ_{pl} = 1.12 S.m^{-1}) of the control volume and the plasma respectively, h is the haematocrit expressed as a fraction and C is a factor that depends on the geometry, deformation and orientation of the RBC at location r (see [15] for further details).

The deformation of a RBC is accounted for by using the deformed short to long axis ratio of (4) in calculating C. To incorporate the orientation effect, C relies on the fraction of aligned cells, $f(r)$ and the fraction of randomly oriented cells. The calculation of C based on the fraction of aligned cells is introduced in this study in (6).

$$C(r) = f(r)\cdot C_b + (1-f(r))\cdot C_r \quad (6)$$

Where C_b and C_r are the C values for aligned and randomly aligned cells respectively.

Step 5. The bulk conductivity of blood shown in (7) is calculated by a summation of the control volume conductivities over the cross section and Ohm's Law as proposed in [15].

$$\sigma_{bl}\ (S.m^{-1}) = \frac{2}{R^2}\int_0^R \sigma_{cv}(r) r\,\mathrm{d}r \quad (7)$$

The impedance, Z was calculated knowing the geometry of the tube set up using (8), where L (m) is the length of the tube under measurement and $A = \pi R^2$ (m^2) is the cross sectional area of the tube.

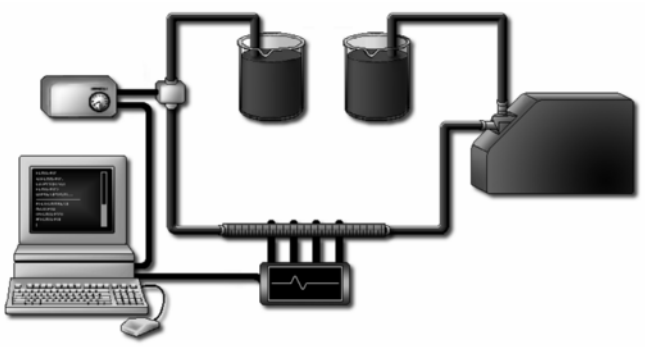

Fig. 1 Mock Circulatory System Experimental Setup

$$Z\ (\Omega) = \frac{L}{A \cdot \sigma_{bl}} \tag{8}$$

B. Experimental Measurements

Eight litres of bovine blood were pumped through rigid tubes from one reservoir to another, as shown in Figure 1. The blood was pumped through silicon tubing using the Harvard Apparatus Pulsatile Blood Pump for Large Animals and Hemodynamic Studies. The impedance was measured in a Perspex rigid tube (12.7 mm diameter) with 4 platinum electrodes using an Impedimed Imp^{TM} SFB7. This device was modified to make rapid measurements at 1 ms intervals for a period of up to 30 seconds at a single current frequency. The impedance was measured at a frequency of 5 kHz. Flow rate was measured by a Transonic ME13 PXN Inline Sensor and TS410 Tubing flow meter. The temperature of the blood was maintained at (23±0.5) ^{o}C and the haematocrit of the blood was measured.

III. Results

Figure 2 shows the theoretically modelled impedance for a single pulse and tube of 12.7mm diameter. The modelled pulse rate was 70 beats per minute (bpm) and haematocrit was 45% to represent physiological conditions. The pulsatile spatial average velocity is shown by the dashed line and the modelled impedance is shown by the dot dashed line.

Figure 3 shows the experimental results collected for flowing bovine blood. This data was collected for the same parameters as those modelled and was averaged over 10 pulses. The measured average velocity is shown by the dashed line and the measured impedance is shown by the dot dashed line.

Results collected over a range of cardiac parameters such as pulse rate, stroke volume and systolic/diastolic ratios demonstrate similar characteristics.

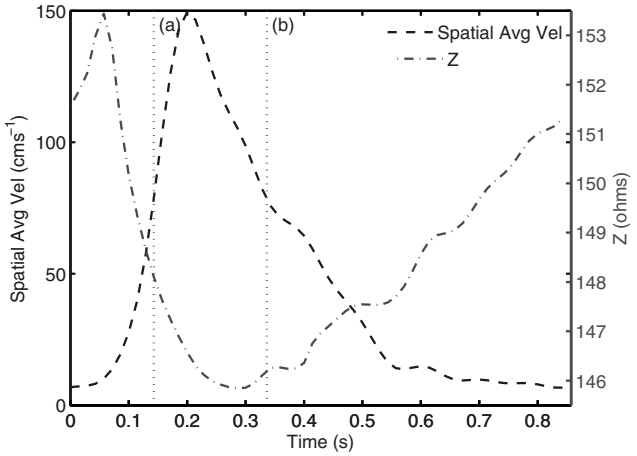

Fig. 2 Modelled absolute spatial average velocity and impedance of blood over one cardiac cycle, h = 45 %, d = 12.7 mm, pulse rate = 70 bpm.

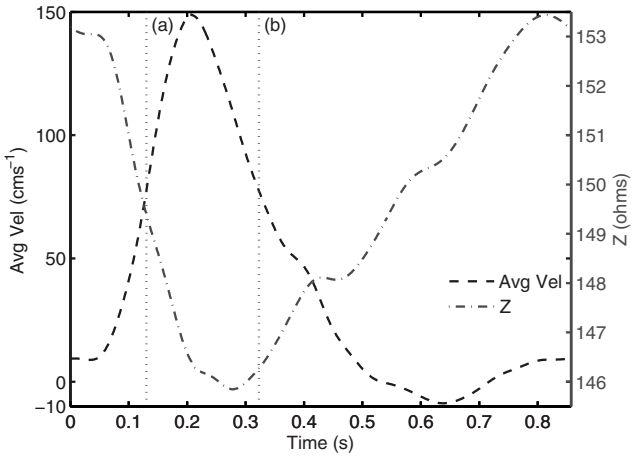

Fig. 3 Experimental average velocity and impedance of blood over one cardiac cycle, h = 45 %, d = 12.7 mm, pulse rate = 70 bpm, freq = 5 kHz.

IV. Discussion

Comparison of the presented results shows that the magnitude and shape of the modelled and experimental impedance waveforms are comparable. In addition, both theoretical and experimental results show similar characteristics. Both results show that changes in the average velocity of blood affects the impedance. The cross correlation between two time series (for zero delay) of velocity and impedance was calculated at 0.73 (theoretical) and 0.65 (experimental). This indicates that impedance waveforms contain information relating to the velocity of blood.

During the acceleration phase (0.08-0.21 s), a strong linear relationship between the average velocity and the im-

pedance is seen (r^2 = 0.95 and 0.98 for theoretical and experimental results respectively). However, during the deceleration phase (0.21s to end of cycle), a decay is evident in impedance response to changes in average velocity. In addition, the impedance is also different between acceleration and deceleration at the same velocity, for example, at times (a) & (b), indicated in Figure 2 and 3 by the vertical dotted lines. This is suggested to be due to differences in velocity profile at these times.

Published stop flow experiments in [8] report that impedance responds instantaneously to increases in velocity, and decays when flow is stopped. Both the modelled and experimental results of the present study demonstrate this as the impedance shows a linear relationship with velocity during acceleration. During the end of the deceleration phase, the impedance is still changing despite the flow having returned to zero. This decay effect is also seen earlier in the deceleration phase when the impedance is less than that for accelerating blood at the same velocity such as at time (b) in comparison to time (a) in both Figure 2 and 3.

This highlights that the relationship between the average velocity and impedance changes during acceleration and deceleration. Understanding this relationship may lead to better understanding of the physiological origins of impedance variations in Impedance Cardiography.

V. Conclusion

It has been experimentally and theoretically shown that impedance of pulsatile blood flowing through rigid tubes varies with the velocity of the blood. This implies that information indicative of the velocity of blood may be contained with in impedance waveforms and may prove useful in Impedance Cardiography.

Acknowledgment

The authors would like to thank Impedimed Pty Ltd for the use of the modified Imp^{TM} SFB7 and technical support.

References

1. R. P. Patterson (1989) Fundamentals of impedance cardiograhy. *Engineering in Medicine and Biology Magazine, IEEE*, 8:35-8
2. L. Wang and R. Patterson (1995) Multiple sources of the impedance cardiogram based on 3-D finite difference human thorax models. *IEEE Trans Biomed Eng* 42:141-8
3. L. A. H. Critchley (1998) Impedance cardiography: the impact of new technology. *Anaesthesia* 53:677-684
4. R. K. Kauppinen, J. A. Hyttinen, and J. A. Malmivuo (1998) Sensitivity distributions of impedance cardiography using band and spot electrodes analyzed by a three-dimensional computer model. *Ann Biomed Eng* 26:694-702
5. F. Skrabal, H. Mayer, E. Hopfgartner, G. Gratze, G. Haitchi, and A. Holler (2005) Multi-site-frequency electromechanocardiography for the prediction of ejection fraction and stroke volume in heart failure. *Eur J Heart Fail* 7:974-83
6. G. Cotter, A. Schachner, L. Sasson, H. Dekel, and Y. Moshkovitz (2006) Impedance cardiography revisited. *Physiol Meas*, 27:817-27
7. K. R. Visser, R. Lamberts, and W. G. Zijlstra (1988) Origin of the impedance cardiogram. VOL 2, *10th Annu. Int. Conf. of the IEEE Engineering in Medicine and Biology Society,* pp. 763-65.
8. K. R. Visser (1989) Electric properties of flowing blood and impedance cardiography. *Ann Biomed Eng*, 17:463-73
9. P. M. de Vries, J. W. Langendijk, and P. M. Kouw (1995) The influence of alternating current frequency on flow related admittance changes of blood: a concept for improvement of impedance cardiography. *Physiol Meas* 16:63-9
10. F. M. Liebman, J. Pearl, and S. Bagno (1962) The electrical conductance properties of blood in motion. *Phys Med Biol* 7:177-94
11. F. M. Liebman and S. Bagno (1968) The behaviour of red blood cells in flowing blood which accounts for conductivity changes. *Biomed Sci Instrum* 4:25-35
12. J. W. Dellimore and R. G. Gosling (1975) Change in blood conductivity with flow rate. *Med Biol Eng* 13:904-13
13. K. Sakamoto and H. Kanai (1979) Electrical characteristics of flowing blood. *IEEE Trans Biomed Eng* 26:686-95
14. K. R. Visser (1992) Electric conductivity of stationary and flowing human blood at low frequencies. *Med Biol Eng Comput* 30:636-40
15. A. E. Hoetink, T. J. C. Faes, K. R. Visser, and R. M. Heethaar (2004) On the flow dependency of the electrical conductivity of blood. *IEEE Trans Biomed Eng* 51:1251-61
16. E. Raaijmakers, J. T. Marcus, H. G. Goovaerts, P. M. J. M. de Vries, Th. J. C. Faes, and R. M. Heethaar (1996) The influence of pulsatile flow on blood resistivity in impedance cardiography. *18th Annu. Int. Conf. of the IEEE Engineering in Medicine and Biology Society*, pp 1957-8.
17. D. A. McDonald (1974) *Blood Flow in Arteries.* Edward Arnold Publishers Ltd , London, pp 17-173
18. M. Zamir (2000) *The Physics of Pulsatile Flow*. Springer-Verlag, New York, pp. 1-112
19. M. Bitbol and F. Leterrier (1982) Measurement of erythrocyte orientation in a flow by spin labelling. *Biorheology* 19:669-80
20. M. Bitbol and D. Quemada (1985) Measurement of erythrocyte orientation in flow by spin labeling II – phenomenological models for erythrocyte orientation rate. *Biorheology* 22:31-42

Address of the corresponding author:

Author: R.L. Gaw
Institute: Queensland University of Technology
Street: 2 George St
City: Brisbane, Queensland
Country: Australia
Email: r.gaw@qut.edu.au